JOURNAL OF MECHANICAL ENGINEERING AND SCIENCES (JMES)
ISSN: 2289-4659 e-ISSN: 2231-8380
VOL. 15, ISSUE 2, 7936 – 7947
DOI: https://doi.org/10.15282/jmes.15.2.2021.01.0626

ORIGINAL ARTICLE

Convective heat transfer and fluid flow characteristics in fin and oval-tube heat exchanger

Y. Abdoune[1], D. Sahel[1,2], R. Benzeguir[1] and K. Alem[1]

[1] Laboratoire des Carburants Gazeux et Environnement (LCGE), Faculté de Génie Mécanique, Université des Science et de Technologie d'Oran Mohamed Boudiaf, 31000, Oran, Algeria
Phone: +213 663125080; Fax: +213 041518811
[2] Département des Sciences Techniques, Université Amar Telidji, Laghouat, 03000, Algeria

ABSTRACT – The forced convective heat transfer behavior of a turbulent air flow, steady and Newtonian over a fin and oval-tube heat exchanger has been examined numerically. Where, the effect of the tube tilt angle (α) on the heat transfer coefficient and the friction factor was tested. The inclination angle of the oval-tubes going from 0° (Baseline case) to 90° with a step of 10°. The fluid flows and heat transfer characteristics are presented for Reynolds numbers ranging from 3.000 to 12.000. All investigations are carried out with the help of the *CFD ANSYS* Fluent. Heat transfer coefficient results in the term of the Nusselt number are validated with the available experimental data and a maximum deviation of 9 % is observed. Reasonable agreement is found. The obtained results show that the tube's inclination angle of 20° is the best design which significantly removes the hot spots behind the tubes, thus giving an increase in the heat transfer coefficient of 13 % compared to the baseline case. In addition, useful correlations are developed to predict Nusselt number and friction factor in the fin and oval-tube heat exchanger.

ARTICLE HISTORY
Received: 03rd Mar 2020
Revised: 10th Oct 2020
Accepted: 05th Jan 2021

KEYWORDS
Heat transfer; oval tube; Nusselt number; friction factor; correlations

INTRODUCTION

Fin and tube heat exchanger (*FTHE*) is a primordial device commonly used in several industrial processes such as thermal centrals, air conditioning systems, refrigerators, automobile radiators and other systems. The thermal performance of fin and tube heat exchanger is limited by using the gases fluid flow such as air. Where, for liquid fluid flow compared with airflow and phase change heat exchangers, the resistance of air side heat transfer convection is usually dominant due to the air thermo-physical properties because heat transfer coefficients are generally inferior for the gas side than for liquid [1–2].Therefore, for better concept to improve the thermal and hydrodynamic characteristics, it is required to set into consideration the influence of the thermo-physical properties of fluid flow, and the geometrical arrangement of heat exchangers. Among the successful techniques of improving the heat transfer execution of gas-side is using vortex generators (*VGs*). The *VGs* are constructed in order to intense the turbulence, thermal and hydrodynamic boundary-layers destruction; heat transfer performance is improved due to these effects. The researches which analyzed the effects of *GVs* on the *FTHEs* thermal performance are very available in literature [3–4].

In this field, several experimental and numerical studies reported that the insertion of *GVs* inside the *FTHEs* helps to guide the fluid flow toward the tubes, intense the speed fluctuations and as a consequence, augments the heat transfer coefficients in the regions behind of the tubes [5–7].Unfortunately, the augmentation of heat transfer rates in the *FTHEs* with *GVs* associates a pressure drop penalty due to the generation of vortex and the changes in the flow direction [8–9]. Fiebig [10] analyzed the effect of winglets vortex generators on the fluid flow and heat transfer behaviors in a fin and tube heat exchanger. The inline and staggered configurations of tubes have been examined. They reported that for the inline tube configuration, the *VGs* increase the heat transfer by 55–65% with a corresponding increase of pressure drop of about 20–45%. He et al [11] numerically studied the effect of a pair of winglets vortex generators for three attack angles (β = 10°, β = 20°, β = 30°). They reported that the winglets with discontinuous rows present a significant increase of heat transfer rates tend to 33.8-70.6%, but also it generates a friction factor penalty of 43.4-97.2% compared with the tubes without *GVs*. The shape of tubes is another important aspect which influence directly on the thermal performance of *FTHEs*. The circular tubes shape presents the classical configuration that was used in the *FTHEs* concept. In 1972, Zukauskas [12] experimentally effected an extensive analysis of fluid flow and heat transfer characteristics over circular tubes banks. Many configurations and thermos-physical proprieties have been analyzed such as the tubes arrangement and flow regime. He elaborated correlations to predict heat transfer coefficients and friction factor and reported that the optimal tubes' arrangement is one of the primordial problems in the design of heat exchangers. Currently, some authors analyzed different tubes shapes such as elliptic [13–15], flat [16–18] and oval [19–21] forms. For examples, Katkhaw et al [13] experimentally investigated the heat transfer performance of external air flow over the ellipsoidal dimple surface with different arrangements and pitch values. The velocity of air stream ranges from 1 to 5 m/s. They found that for staggered arrangements, the dimpled surfaces with a pitch of (S_L/D_{minor} = 1.875) and Spanwise pitch to Dimple diameter

*CORRESPONDING AUTHOR | Y. Abdoune | yamina.abdoune@univ-usto.dz

on minor axis (S_T/D_{minor} =3.125), gives the optimum thermal resistance values of about 15.8% better than the smooth plate. For inline arrangements, S_L/D_{minor} = 1.875 and S_T/D_{minor} = 1.875 show the optimum thermal heat transfer coefficients about 21.7% better than the smooth plate. Based on the results obtained correlations were reported for both inline and staggered configurations. In order to test a steady air laminar flow side in a channel of a flat tube with dimpled fin, Wei et al [17] show that dimpled fin has better heat transfer performance than the plain fin. It was observed that whenever the same intensity of secondary flow is produced by increasing dimple radius, the dimple pitch and the fin spacing, the same heat transfer intensity is obtained. Ishak et al [21] experimentally examined the heat transfer performance of airflow in a staggered flat tube bank in crossflow with laminar-forced convection. The Reynolds number range from 373 to 623 and the total heat flux varied from 967.92 to 3629.70 W/m^2. They found that in the Reynolds numbers varied from 373 to 623 for the fixed heat flux, the mean Nusselt number for all the flat tubes is increased by 11.46–46.42%. The average Nusselt number increased between 21.39–84% for a Re = 498 and the heat flux supply ranges between 967.9 to 3629.7 W/m2. A new Nusselt number-Reynolds number correlation was determined. Alireza et al [22], investigated experimentally and numerically the heat transfer performance and pressure loss of a finned oval tube heat exchanger to study the effects of fin length, fin spacing and diameter ration of the tube cross section. In order to find the optimum arrangement, they found that for low Reynolds number the fin spacing of 1 mm shows the best results at all tubes aspect ratios and fin lengths. Zhu et al [23], studied the effect of ellipticity of two tubes in two rows fin-and-tube heat exchanger in staggered arrangement for different Reynolds numbers by performing a three-dimensional numerical simulation combined with an artificial neural network (*ANN*) and Multi-objective genetic algorithm (*MOGA*). In addition, they showed that lower elliptic tube followed by higher elliptic tube has better thermal and hydraulic performance than other configurations [24–25]. Tang et al [26] experimentally studied the effect of various air inlet angles on the heat transfer and flow friction characteristics of a tow-row plain finned oval tube heat exchanger. They showed that air inlet angle of 45° provided the best heat transfer performance compared with the others angles. In order to investigate the effect of tube shape on air-side performance of *FTHE* under typical conditions, varying both dry bulb temperature and air flow velocity, Shiquan et al [27] observed that air flowing outside elliptic tube showed much better heat transfer coefficient with 66% higher than that circular tube. In the same context, other parameters need to be analyzed such as tubes pitch ratios (*PR*) [28], and ellipticity ratios (*b/a*) [29].

In 2015, and in an extensive research, Tahseen et al [30] displayed several papers which are relevant to the tube banks heat exchangers. They reported that the heat transfer and pressure drop characteristics of *FTHEs* depend on various parameters. They summarized these parameters as follows: velocity of external fluid, tubes rows, tube arrangement (in-line/staggered, series), tube spacing, fin spacing, form of tubes. In addition, among some recommendations, they advised that tubes shape such as the flat and elliptic forms merit to be used in the *FTHEs* design.

In this context, some authors have described that many correlations need to be corrected by considering other parameters such as the tube size, and the longitudinal tube ratios [31] and other shapes [32–33]. These last recommendations encouraged us to consider the effect of a new parameter in this paper. It concerns the impact of the inclination of the oval tubes on the thermal and hydrodynamic performances of a *FTHE*. Based on numerical results, reliable correlations have been proposed to predict heat transfer coefficients and friction factors. Where, these correlations provide a necessary basis for *FTHEs* design.

PHYSICAL AND NUMERICAL MODELS

FTHE and Oval Tubes Configurations

The numerical analyses are realized by the computer code Ansys Fluent. The geometry of the problem analyzed as a numerical domain is shown in Figure 1(a) and 1(b). It consists of a fin and oval-tubes heat exchanger. The investigations based on the test of tube's inclination angle (α), which is varied from 0° to 90°, with 10° of step. The tube configuration is exposed in Figure 1(b). The longitudinal/transversal diameters ratio (D_a / D_b) of the oval tube is 2, the transverse tube pitch (S_T) is 42.20 mm, and the longitudinal tube pitch (S_L) is 31.65 mm. Considering the Reynolds number interval (3.000 to 12.000) and the tube's inclination angle (0° to 90°), fifty cases were analyzed in this investigation.

Physical Conditions and Mathematical Formulation

The regime of fluid flow is characterized in the inlet with Reynolds number varying from 3.000 to 12.000. The air flow regime is considered turbulent and incompressible. A steady state is assumed for the perdition of fluid flow and heat transfer. The air thermo-physical properties are supposed constant. A constant temperature is supposed for the oval tube wall. Also, the radiation heat transfer is neglected. The continuity, momentum and energy equations are the governed equations which are used to predict the airflow and heat transfer inside the heat exchanger, these equations expressed as follows:

Continuity equation:

$$\frac{\partial}{\partial x_i}(\rho u_i)=0 \tag{1}$$

Momentum equation:

$$\frac{\partial}{\partial x_i}\left(\rho u_i u_j\right)=\frac{\partial}{\rho x_i}\left[\mu\left(\frac{\partial u_i}{\partial x_j}-\overline{\rho u_i^{'} u_j^{'}}\right)\right]-\frac{\partial P}{\partial x_i} \tag{2}$$

Energy equation:

$$\frac{\partial}{\partial x_i}\left(\rho u_i T\right)=\frac{\partial}{\rho x_i}\left(\left(\Gamma+\Gamma_t\right)\frac{\partial T}{\partial x_j}\right) \tag{3}$$

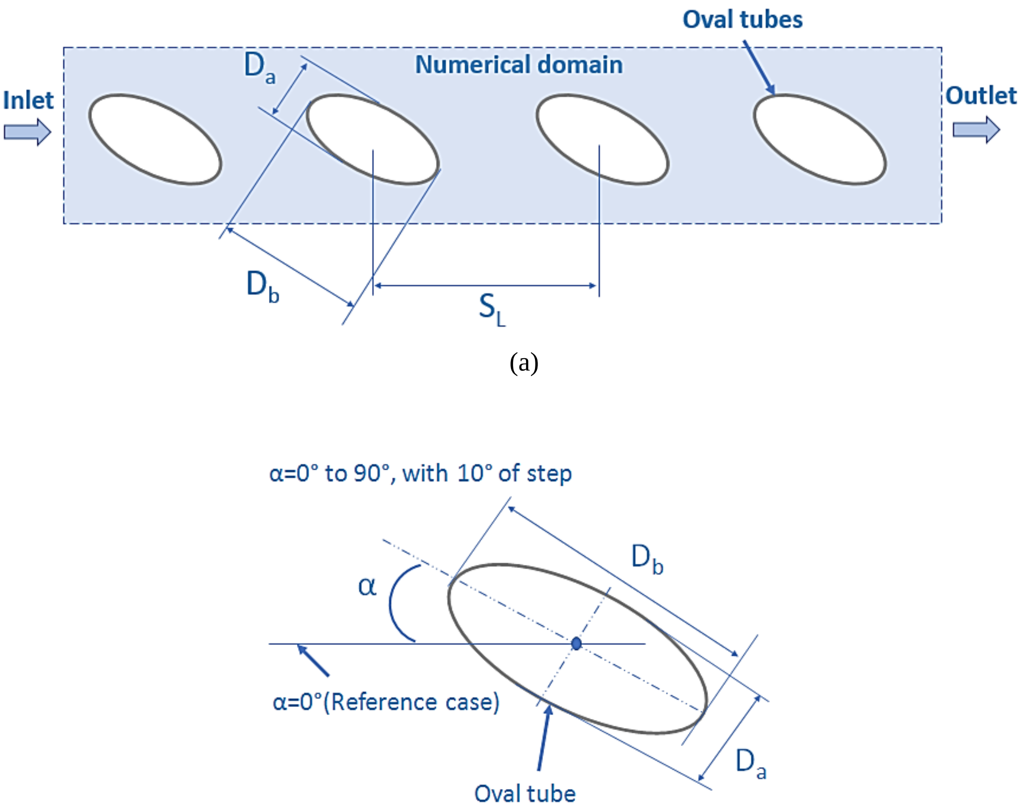

(a)

(b)

Figure 1. Configurations of: (a) a fin-and-oval-tube heat exchanger with (b) different tubes inclination angle (α)

where Γ is the molecular thermal diffusivity, Γ_t is the turbulent thermal diffusivity:

$$\Gamma=\mu/Pr\,;\ \Gamma_t=\mu_t/Pr_t\ ;\ \mu_t=\rho C_\mu(k^2/\varepsilon) \tag{4}$$

$\overline{\rho u_i^{'} u_j^{'}}$ are the Reynolds stresses defined by the Boussinesq hypothesis:

$$\overline{\rho u_i^{'} u_j^{'}}=\mu_t\left(\frac{\partial u_i}{\partial x_j}+\frac{\partial u_i}{\partial x_i}\right)-\frac{2}{3}\left(\rho k+\mu_t\frac{\partial u_i}{\partial x_j}\right)\delta_{ij} \tag{5}$$

where, δ_{ij} is the Kronecker delta.

In order to close of the equations, the *RNG k-ε* model of turbulence which is based on the turbulent kinetic energy k (Eq. 6*)* and the energy dissipation ε (Eq. 7) is used in this study. This model is largely utilized to predict the turbulent flow and heat transfer inside heat exchangers [32].

$$\frac{\partial \rho}{\partial x_i}(\rho k u_i)=\frac{\partial}{\partial x_j}\left[\left(\mu+\frac{\mu_t}{\sigma_k}\right)\frac{\partial k}{\partial x_j}\right]+P_k-\rho\varepsilon \tag{6}$$

$$\frac{\partial \rho}{\partial x_i}(\rho \varepsilon \upsilon_i)=\frac{\partial}{\partial x_j}\left[\left(\mu+\frac{\mu_\tau}{\sigma_\varepsilon}\right)\frac{\partial \varepsilon}{\partial x_j}\right]+C_{1\varepsilon}\frac{\varepsilon}{\kappa}\Pi_\kappa-C^*_{2\varepsilon}\,\rho\,\frac{\varepsilon^2}{k} \tag{7}$$

Where, G_k represents turbulence kinetic energy generated by the mean velocity gradients.

$$C^*_{2\varepsilon}=C_{2\varepsilon}+\frac{C_\mu \eta^3(1-\eta/\eta_0)}{1+\beta\eta^3} \tag{8}$$

P_k is the production term of the turbulent kinetic energy due to the mean velocity gradient. It is defined as: $P_k=\mu_t S^2$

Where S is the modulus of mean rate of strain tensor, defined as: $S=\left(2S_{ij}S_{ij}\right)^{1/2}$

The constants of the *RNG k-ε* turbulence model are valued as: $C_{1\varepsilon}=1.42$, $C_{2\varepsilon}=1.68$, $\eta=Sk/\varepsilon$, $\eta_0=4.38$, $\beta=0.012$.

Governing Parameters

In the heat exchanger, the efficiency of governed parameters considerably related to the geometry of heat exchanger and fluid flow conditions. The flow regime can be determined by Reynolds number, bulk temperature, average, or local heat transfer coefficient. The better heat exchanger design is combined between the highest heat transfer rate and the least pressure loss. In the present analyzes, the Nusselt number, friction factor are the fundamental parameters which are used to explain the thermal and hydrodynamic behaviors of *FTHEs*. The velocity, temperature are additional parameters leading to a supplementary understanding of the physical phenomena. These dimensionless parameters are determined as follows:

Reynolds number:

$$Re=\frac{\rho U_m D_h}{\mu} \tag{9}$$

Where μ is dynamic viscosity, U_m is mean velocity at the minimum flow cross-sectional, ρ is density and D_h is the hydraulic diameter.

Total heat transfer coefficient:

$$Q=m_f C_p\left(T_{out}-T_{in}\right) \tag{10}$$

Where m_f is mass flow rate, C_p is specific heat and T is temperature of inlet and outlet.

The logarithmic mean temperature difference:

$$\Delta T_{lm}=\frac{\left(\left(T_{wall}-T_{in}\right)-\left(T_{wall}-T_{out}\right)\right)}{ln\left(\frac{\left(T_{wall}-T_{in}\right)}{\left(T_{wall}-T_{out}\right)}\right)} \tag{11}$$

The heat transfer coefficient given as:

$$h=\frac{Q}{A.\Delta T_{lm}} \tag{12}$$

Where A is total heat transfer surface area.

Nusselt number:

$$Nu=\frac{h D_h}{k} \tag{13}$$

Where k is thermal conductivity.

Friction factor along the test section given as:

$$f = \frac{\Delta P}{\frac{1}{2}\left(\rho U_m^{\ 2}\right)} \tag{14}$$

Where, ΔP is the pressure difference between inlet and outlet is assumed as:

$$\Delta P = P_{in} - P_{out} \tag{15}$$

Boundary Conditions

For the tube's walls, a no-slip boundary condition was performed, where both components of velocity were set to zero. These walls were maintained to constant wall temperature ($T_w = 350°K$). The profiles of temperature and velocity are recognized at the inlet air flow passage section. A uniform velocity ($U = U_{\text{in}}$) and a constant temperature ($T_{in} = 300$ °K) are utilized in the inlet section. At the outlet section, the conditions of Neumann boundary are utilized for all variables, thus the streamwise variable gradients are fixed to be zero.

Grid Independence Strategy

Before analyzing the impacts of oval-tubes arrangement on the heat transfer and fluid flows characteristics, it is essential to adopt an appropriate meshes system for calculations which is leading to a correct physical result. The Computational Fluid Dynamics (*CFD*) Ansys Fluent is employed to investigate the fluid flows and heat transfer in the *FTHE*. Meshes of the computational domain were created by using the Gambit software 2.4.6. A number of tests grid series were realized on all numerical domains. A triangular grid type, no-uniform is selected. A refined mesh density is used near the walls of tubes in order to predict the temperature and velocity gradients. The meshes selected in the Baseline case ($\alpha = 0°$) with *Re* = 5000 are 61.249, 87.998, 100.915, 134.014 and 160.118. It was found that the deviations of the Nusselt numbers results did not exceed 1.8 % when the grid number is higher than 100.615 cells. Thus, the grid of 100.615 cells was utilized to check the soundness of the present computer code. Likewise, for this grid series, Figure 2(a) and 2(b) displays the distribution of the temperature and velocity gradients at x=0.08 m, and remarkable stability of the tow profiles distributions is observed. The same approach was then utilized to test the grid independence for the other tube's inclination angles. The method of finite volume is used to solve the Navier–Stokes and energy equations. The convective terms in governing equations for momentum and energy are discretized with the first upwind scheme. The *SIMPLE* algorithm (*Semi-Implicit Method for Pressure- Linked Equations*) is used to perform the velocity-pressure coupling. For the convergence, Default under-relaxation factors of the Fluent solver are implemented. The convergence criterions for the normalized residuals are fixed at 10^{-5} for the flow equations and 10^{-9} for the energy equation. The numerical investigations are achieved on a PC-i5 with a *CPU* frequency of 2.5 Go and a *RAM* of 6 Go. A typical running time for calculation of a case is about four to seven minutes.

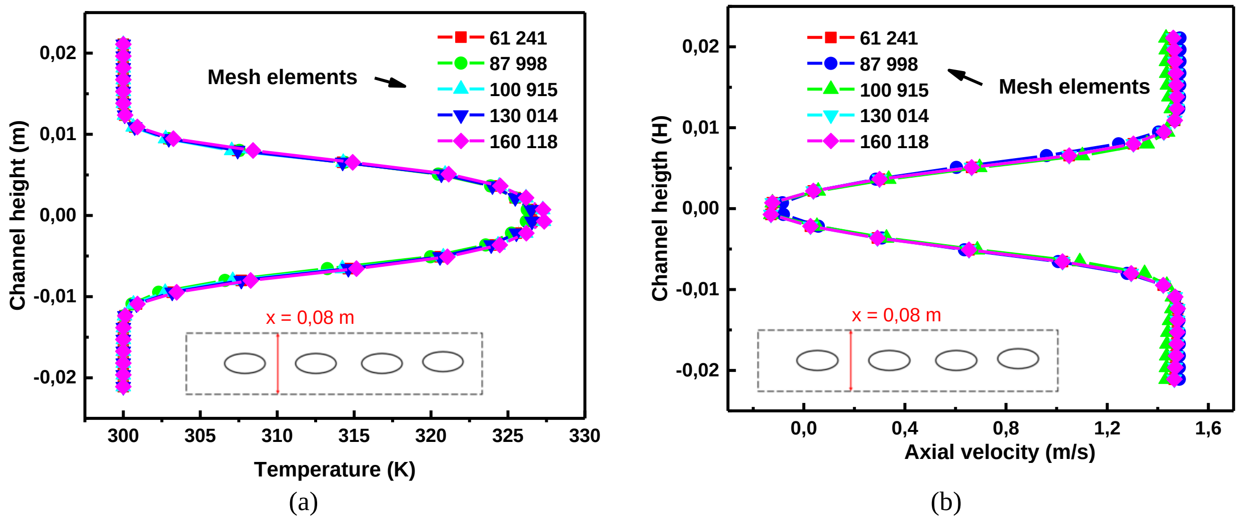

Figure 2. Distribution of: (a) temperature and (b) axial velocity, at x = 0.08 m, *Re*=5.000

RESULTS AND DISCUSSIONS

Validation of Results

For precise results, it is required to check the reliability of the *CFD* code used in this investigation. For this purpose, we based on the experimental study realized by Baoxing and Zuhui [34] and we realized the same geometrical arrangements. Another comparison was achieved with the work of Zhao et al [35]. For different values of Reynolds number, the numerical results for Nusselt number and friction factor are illustrated in Figure 3. The comparison between our numerical results, the experimental data reported by Baoxing and Zuhui [34] and those of Zhao et al [35] is conducted in this section. Where, comparison with Baoxing and Zuhui data [34], maximum deviations of 9 % and 10 % are observed for both Nusselt number and friction factor, respectively. The evaluation with ref [35], extreme deviations of 8% and 5 % are quantified for the same parameters and conditions.

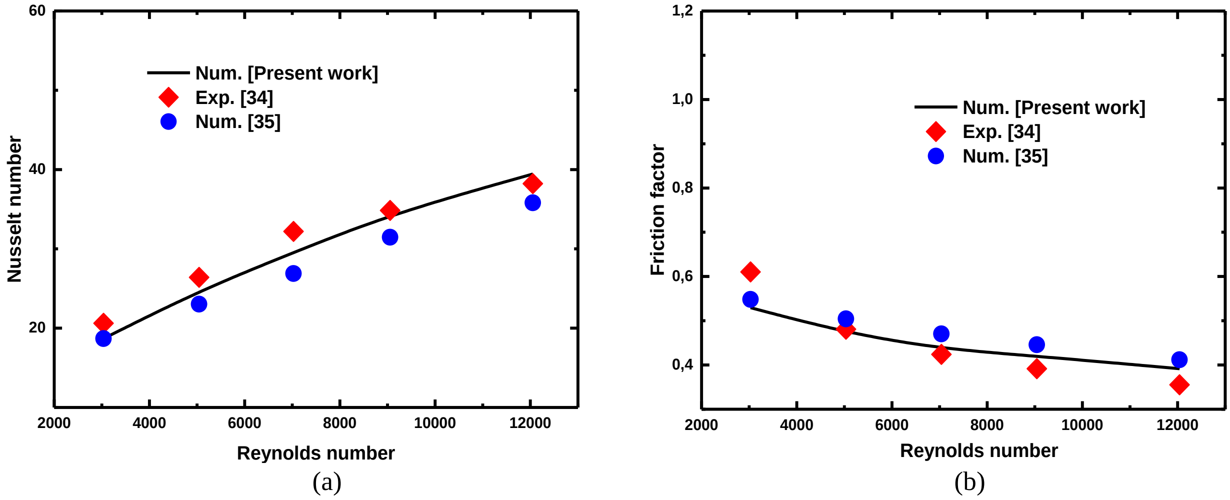

Figure 3. Comparison of: (a) Nusselt number and (b) friction factor results

Hydrodynamic and Thermal Aspects of Air Flow

From literature, it is known that the major problem in using circular tubes in heat exchangers is the formation of hot points behind these tubes. For an external flow of tubes, the formation of fluid recirculation zones behind the tubes with low speeds causes hot points (or pockets) which is reduces the heat transfer coefficient in these zones. In this context, the increase in speed fluctuations behind the tubes is one of the main reasons for improving the performance of heat exchangers. The axial velocity contours present a useful physical parameter leading to a correct understanding of physical phenomena. Figure 4 shows the distribution of axial velocity for all cases studied in this work. The stagnation of the fluid flow after the tubes is obviously appearing in the case of tubes with inclination angles.

In the range of 0° to 20°, the area of the fluid recirculation starts to be reduced as the attack angle increases, reaching its small area in the case of the inclination angle of 20°. From the angle 30°, the areas of airflow stagnation appear at a large surface behind the tubes, where the main flow passes on the extremities of the oval-tubes. In these cases (30° to 90°), the flow separates into two large regions; the first presents a large quantity of the flow which passes at high speed on the upper and lower sides of the tubes.

The second region behind the tubes is caused by the separation of the main flow at the extremity of the tubes. The latter is an undesirable phenomenon on the heat transfer performance, where the stagnated areas of the fluid flow cause the formation of hot pockets, and as a result, it reduces the heat transfer coefficient. There is a fundamental relationship between the formation of low velocity zones or stagnant regions and the formation of hot pockets. Where Figure 4 and 5 clearly show this relationship while the fluid structure directly influences the thermal behavior of *FTHEs*. Indeed, the increases in speed fluctuations help to reduce the formation of hot pockets, and as a consequence increases the performance of *FTHE*. Apparently, the 20° angle ensures the weakest fluid stagnation zone compared to other cases, where which is merits to be considered in the *FTHEs* design.

Heat Transfer

As we explained above, the formation of hot points appears obviously between the tubes produced by the stagnant or flow recirculation regions, the heat transfer rate is then reduced. The effects of tubes' inclination angles (α) on the heat transfer is studied in this section. Figure 6 depicts the variations of the Nusselt number versus the tube's inclination angles for various Reynolds number (*Re*) values. This figure shows clearly that the Nusselt number augment according to the increases of the Reynolds number (*Re*) values due to the rise of the velocity fluctuations, turbulence intensity and the rise of inertial shears near the tubes. Between 0° and 20°, the Nusselt number tends to increase according to the tube's inclination angle and reaching its highest value in the case of tube's inclination angle of 20°.

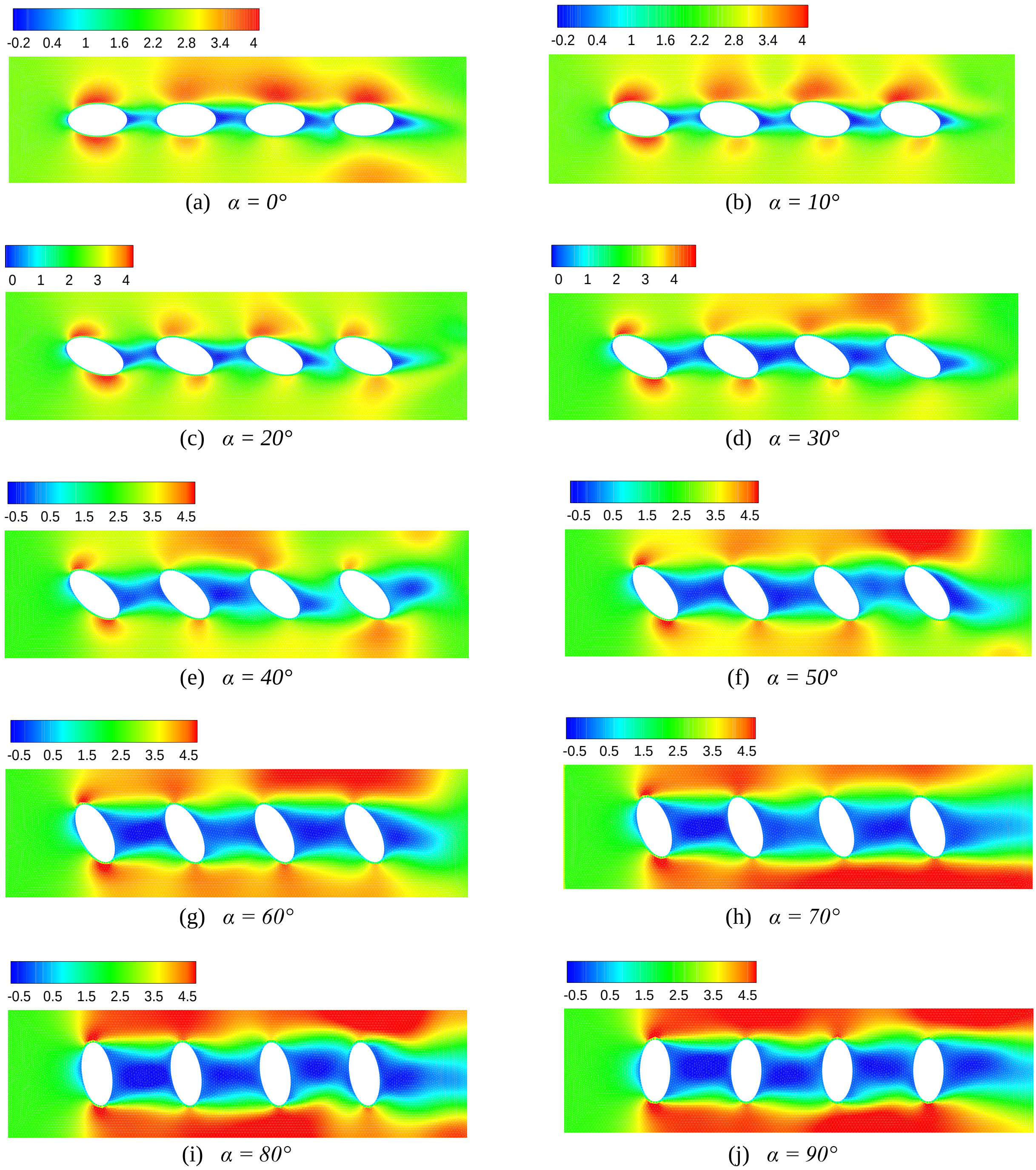

Figure 4. Axial velocity contours for different tubes inclination angle (α), *Re* = 5.000

Beginning the angle of 30°, the Nusselt number tends to decrease versus the angle of the inclination of tubes and attain its feeble values in the cases of 80° and 90°. It is very easy to explain these variations of Nusselt numbers, where the slight inclination of tubes ($\alpha = 20°$) helps to guide the main airflow towards the regions behind the tubes, also it agitates the stagnated flow zones, creates a better flow mixture, and as a consequence, it improves the heat transfer coefficients increase of 13% compared with the baseline case. On the other hand, the diminution of the Nusselt number for 30° to 90° by 4% to 26 % due to the augmentation of the flow recirculation zones and the formation of the hot points behind of the tubes which reduces the heat transfer execution.

Pressure Drops

As each energetic system, the augmentation of heat transfer rates in the *FTHE* associates a pressure drop penalty. In this context, the variations of pressure drop against tubes inclination angle (α) for various Reynolds number (*Re*) values are discussed in this section from Figure 7. This figure displays evidently that the friction factor decreases according to the increases of the *Re* values due to the rise of the velocity fluctuations near the tubes. Also, the friction factor increases versus the rise of the tube's inclination angles ranging from 0° to 20°. The friction factor attains to 2 times upper than that of the baseline case (α= 0°). The rise of friction rate on the large surface and increasing of speed fluctuations are responsible for these augmentations. In the interval of 20° to 90°, the friction factor decreases by about 0.3 to 0.5 times less than that of the baseline case. Where a large quantity of the airflow passes directly on the upper and lower extremities of the tubes due to the separation of the main flow which reduces the pressure drop. The highest value of friction factor in the case of 20° (augmentation of 2 times compared with the baseline case) due to the change in the flow direction and the formation of the vortex between the tubes.

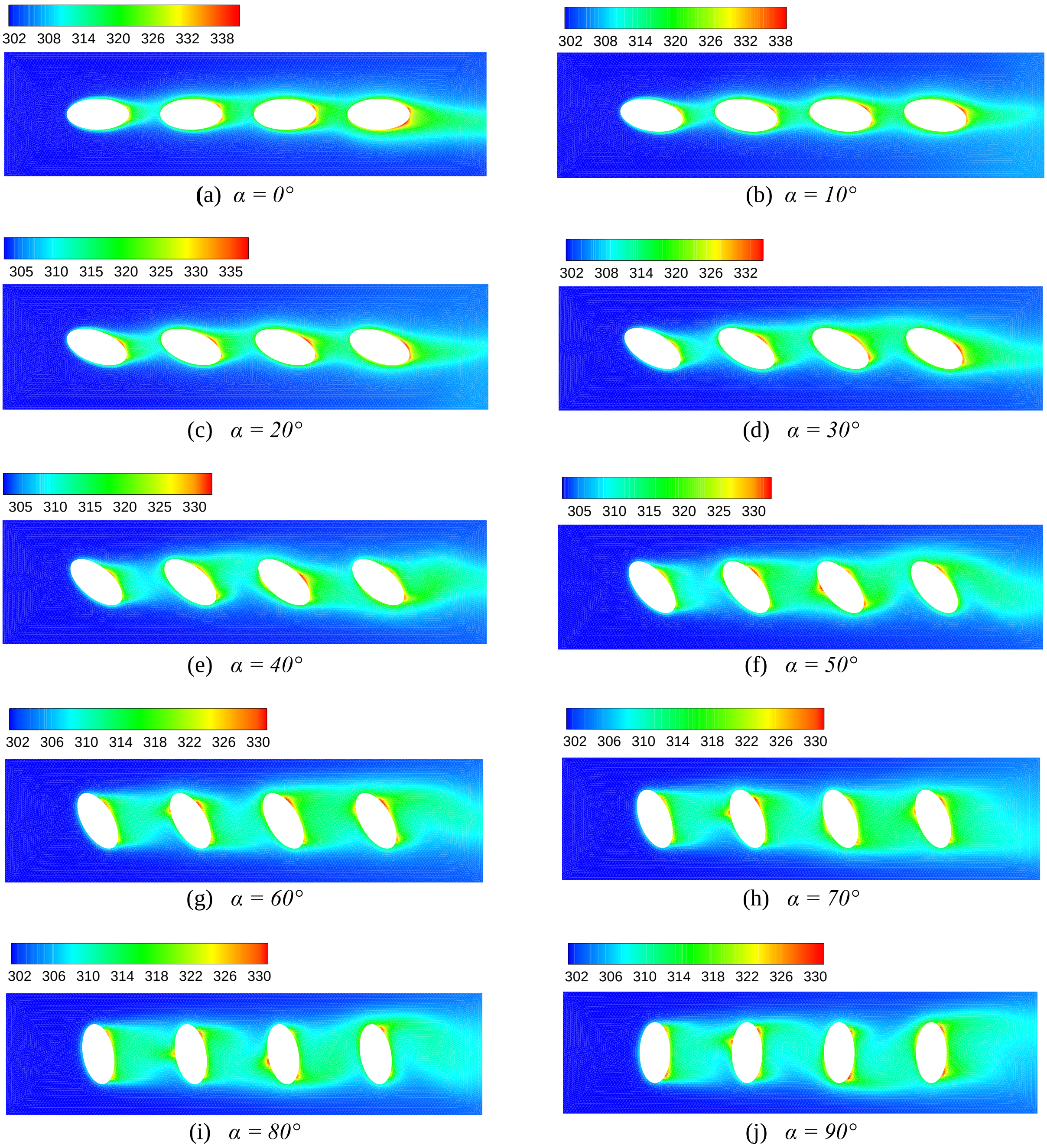

Figure 5. Temperature contours for different tubes inclination angle (α), Re = 5.000

Development of Correlations

On the base of the present results, heat transfer coefficients and friction factor correlations were elaborated using Reynolds numbers and tube's inclination angles. Before elaborate the correlations, it is required to validate the present results, which is performed in Figure 3. In order to assure a high accuracy of correlations, we divided the range of the inclination angle of tubes into two parts: the first part varies from 0° to 30°, and the second varies from 30° to 90°. Indeed, two correlations have been proposed to predict each parameter (Nusselt number and friction factor). Therefore, new correlations for the estimation of Nusselt number (Eqs. (16) and (17)) and friction factor (Eqs. (18) and (19)) depending on Reynolds number and inclination angle of tubes have been elaborated in this section. The predicted data and numerical results are compared as shown in Figure 8(a). All deviations are within 8 %, signifying that the heat transfer correlations are of satisfactory precision. From Figure 8(b), the deviations of friction factor correlations are about 10%, indicating then that these correlations are also of reasonable accuracy. Hence, these correlations may be valuable for the user to estimate the values of Nusselt number and friction factor in such fin and oval-tube heat exchanger without experiments and additional efforts.

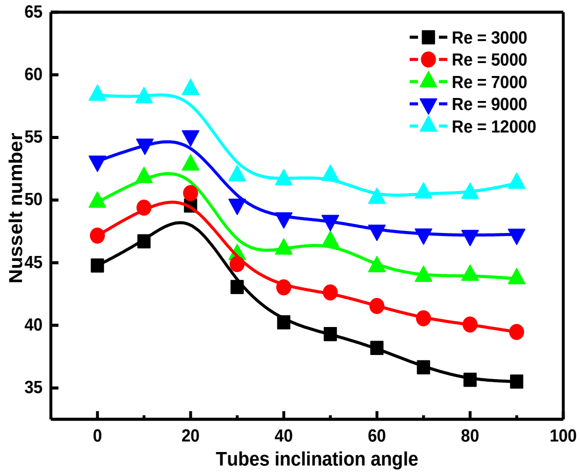

Figure 6. Variation of Nusselt number (*Nu*) versus tubes inclination angle (α), for different Reynolds number (*Re*) values

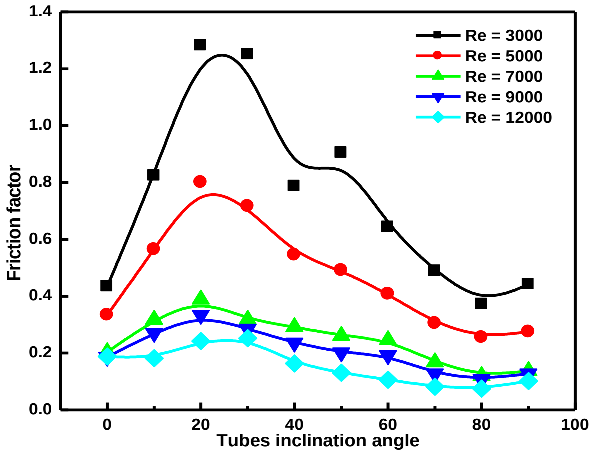

Figure 7. Variation of friction factor (*Nu*) versus tubes inclination angle (α), for different Reynolds number (*Re*) values

$$Nu = \left(-0.0003\ \alpha^3 + 0.0089\ \alpha^2 + 0.0225\ \alpha + 12.4562\right) Re^{0.1562} \tag{16}$$

For $0 \leq \alpha \leq 30°$, and $3000 \leq Re \leq 12000$

$$Nu = 12.1896\ \alpha^{-0.115}\ Re^{0.2006} \tag{17}$$

For $30° \leq \alpha \leq 90°$, and $3000 \leq Re \leq 12000$

$$f = \left(-0.5755\ \alpha^3 + 18.7057\ \alpha^2 + 107.9175\ \alpha + 3879.2744\right) Re^{-1.108} \tag{18}$$

For $0 \leq \alpha \leq 30°$, and $3000 \leq Re \leq 12000$

$$f = 985021.055\ \alpha^{-0.964}\ Re^{-1.274} \tag{19}$$

For $30° \leq \alpha \leq 90°$, and $3000 \leq Re \leq 12000$

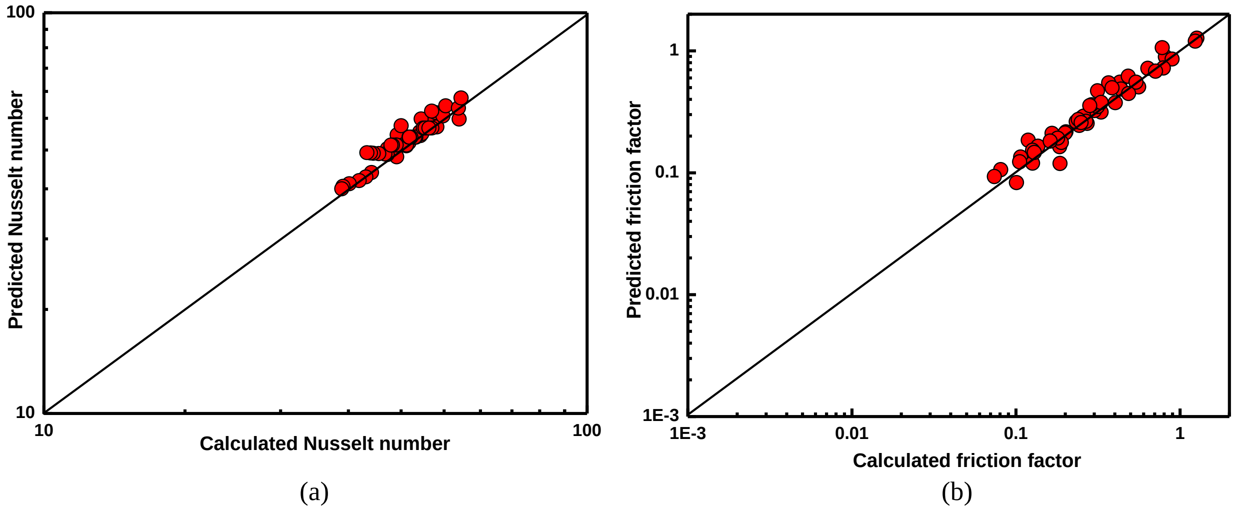

Figure 8. Comparison between predicted results and numerical data of: (a) Nusselt number and (b) friction factor

CONCLUSIONS

A two-dimensional numerical method was utilized to test the performance of fin and oval-tube heat exchangers. The investigation was focused on different values of tube's inclination angle ranging from 0° to 90°. The fluid flows and heat transfer characteristics are analyzed for Reynolds numbers ranging from 3.000 to 12.000. The main conclusions are summarized as follows:

1) Comparing with the baseline case ($\alpha = 0°$), the inclination of the oval tubes enhances considerably the heat transfer, especially in the tube's inclination angle ranging from 10° to 20°, which create an increase of heat transfer coefficients with 5% to 13%.
2) The case of tube's inclination angle of 20° presents the best design that eliminates significantly the hot points behind of the tubes, giving thus an increase in the heat transfer coefficient of 13 % compared with the baseline case ($\alpha = 0°$).
3) The friction factor decreases according to the rises of the *Re* values. Also, the friction factor increases versus the rise of the tube's inclination angles ranging from 0° to 20° and it attains to 2 times upper than that of α=0°. In the interval of 20° to 90°, the friction factor decreases by 0.3 to 0.5 times less than that of the same case.
4) The numerical results allow us to propose reliable correlations to predict Nusselt number and friction factor in the fin and oval-tube heat exchangers.

ACKNOWLEDGMENTS

The authors would like to acknowledge General Directorate for Scientific Research and Technological Development (DGRSDT)- Ministry of Higher Education and Scientific Research of Algeria for its supports.

REFERENCES

[1] B. Anoop, C. Balaji, and K. Velusamy, "A characteristic correlation for heat transfer over serrated finned tubes," *Ann. Nucl. Energy*, vol. 85, pp. 1052–1065, 2015, doi: 10.1016/j.anucene.2015.07.025.

[2] H. Huisseune, S. De Schampheleire, B. Ameel, and M. De Paepe, "Comparison of metal foam heat exchangers to a finned heat exchanger for low Reynolds number applications," *Int. J. Heat Mass Transf.*, vol. 89, pp. 1–9, 2015, doi: 10.1016/j.ijheatmasstransfer.2015.05.013.

[3] D. Sahel, H. Ameur, and Y. Kamla, "A numerical study of fluid flow and heat transfer over a fin and flat tube heat exchangers with complex vortex generators," *Eur. Phys. J. Appl. Phys.*, vol. 78, no. 3, pp. 34805, 2017, doi: 10.1051/epjap/2017170066.

[4] D. Sahel, R. Benzeguir, and T. Baki, "Heat transfer enhancement in a fin and tube heat exchanger with isosceles vortex generators," *Mechanics.*, vol. 21, no. 6, pp. 457-464, 2015, doi: 10.5755/j01.mech.21.6.12240.

[5] S. K. Sarangi and D. P. Mishra, "Effect of winglet location on heat transfer of a fin-and-tube heat exchanger," *Appl. Therm. Eng.*, vol. 116, pp. 528–540, 2017, doi: 10.1016/j.applthermaleng.2017.01.106.

[6] T. Välikangas, S. Singh, K. Sørensen, and T. Condra, "Fin-and-tube heat exchanger enhancement with a combined herringbone and vortex generator design," *Int. J. Heat Mass Transf.*, vol. 118, pp. 602–616, 2018, doi: 10.1016/j.ijheatmasstransfer.2017.11.006.

[7] L. O. Salviano, D. J. Dezan, and J. I. Yanagihara, "Thermal-hydraulic performance optimization of inline and staggered fin-tube compact heat exchangers applying longitudinal vortex generators," *Appl. Therm. Eng.*, vol. 95, pp. 311–329, 2016, doi: 10.1016/j.applthermaleng.2015.11.069.

[8] M. J. Li, W. J. Zhou, J. F. Zhang, J. F. Fan, Y. L. He, and W. Q. Tao, "Heat transfer and pressure performance of a plain fin with radiantly arranged winglets around each tube in fin-and-tube heat transfer surface," *Int. J. Heat Mass Transf.*, vol. 70, pp. 734–744, 2014, doi: 10.1016/j.ijheatmasstransfer.2013.11.024.

[9] S.-Y. Yoo, D.-S. Park, M.-H. Chung, and S.-Y. Lee, "Heat transfer enhancement for fin-tube heat exchanger using vortex generators," *KSME Int. J.*, vol. 16, no. 1, pp. 109–115, 2002, doi: 10.1007/BF03185161.

[10] M. Fiebig, "Embedded vortices in internal flow: heat transfer and pressure loss enhancement," *Int. J. Heat Fluid Flow.*, vol. 16, no. 5, pp. 376–388, 1995, doi: 10.1016/0142-727X(95)00043-P.

[11] Y. L. He, H. Han, W. Q. Tao, and Y. W. Zhang, "Numerical study of heat-transfer enhancement by punched winglet-type vortex generator arrays in fin-and-tube heat exchangers," *Int. J. Heat Mass Transf.*, vol. 55, no. 21, pp. 5449–5458, 2012, doi: 10.1016/j.ijheatmasstransfer.2012.04.059.

[12] A. Žkauskas, "Heat Transfer from Tubes in Crossflow," *Adv. Heat Transf. Elsevier.*, vol. 18, pp. 87–159, 1987.

[13] N. Katkhaw, N. Vorayos, T. Kiatsiriroat, Y. Khunatorn, D. Bunturat, and A. Nuntaphan, "Heat transfer behavior of flat plate having 45° ellipsoidal dimpled surfaces," *Case Stud. Therm. Eng.*, vol. 2, pp. 67–74, 2014, doi: 10.1016/j.csite.2013.12.002.

[14] A. Horvat and B. Mavko, "Drag coefficient and stanton number behavior in fluid flow across a bundle of wing-shaped tubes," *J. Heat Transf.*, vol. 128, no. 9, pp. 969–973, 2006, doi: 10.1115/1.2241746.

[15] A. Horvat, M. Leskovar, and B. Mavko, "Comparison of heat transfer conditions in tube bundle cross-flow for different tube shapes," *Int. J. Heat Mass Transf.*, vol. 49, no. 5, pp. 1027–1038, 2006, doi: 10.1016/j.ijheatmasstransfer.2005.09.030.

[16] A. Horvat and B. Mavko, "Heat Transfer Conditions in Flow Across a Bundle of Cylindrical and Ellipsoidal Tubes," Numer. *Heat Transf. Part Appl.*, vol. 49, no. 7, pp. 699–715, 2006, doi: 10.1080/10407780500496554.

[17] X.-Q. Wei, Y.-H. Zhang, W.-L. Hu, and L.-B. Wang, "The fluid flow and heat transfer characteristics in the channel formed by flat tube and dimpled fin," *Int. J. Therm. Sci.*, vol. 104, pp. 86–100, 2016, doi: 10.1016/j.ijthermalsci.2015.12.018.

[18] N. Benarji, C. Balaji, and S. P. Venkateshan, "Unsteady fluid flow and heat transfer over a bank of flat tubes," *Heat Mass Transf.*, vol. 44, no. 4, p. 445, 2007, doi: 10.1007/s00231-007-0256-5.

[19] T. L. Fullerton and N. K. Anand, "Periodically fully-developed flow and heat transfer over flat and oval tubes using a control volume finite-element method," *Numer. Heat Transf. Part Appl.*, vol. 57, no. 9, pp. 642–665, 2010, doi: 10.1080/10407781003744888.

[20] M. Ishak, T. A. Tahseen, and M. Rahman, "Experimental Investigation on heat transfer and pressure drop characteristics of air flow over a staggered flat tube bank in crossflow," *Int. J. Automot Mech. Eng.*, vol. 7, pp. 900, 2013, doi: 10.15282/IJAME.7.2012.7.0073.

[21] T. A. Tahseen, M. Ishak, and M. M. Rahman, "An experimental study air flow and heat transfer of air over in-line flat tube bank," *in International Conference on Mechanical Engineering Research (ICMER2013)*, 2013, vol. 1, p. 3.

[22] A. Hashem-ol-Hosseini, M. Akbarpour Ghazani, and M. D. Emami, "Experimental study and numerical simulation of thermal hydraulic characteristics of a finned oval tube at different fin configurations," *Int. J. Therm. Sci.*, vol. 151, p. 106255, 2020, doi: 10.1016/j.ijthermalsci.2019.106255.

[23] H. Zhu, Z. Yang, T. A. Khan, W. Li, Z. Sun, J. Du, Z. Zhang, and J. Zhou, "Thermal-hydraulic performance and optimization of tube ellipticity in a plate fin-and-tube heat exchanger," *J. Electron. Packag.*, vol. 141, no. 3, 2019, doi: 10.1115/1.4043482.

[24] L. Zhao, B. Wang, R. Wang, and Z. Yang, "Aero-thermal behavior and performance optimization of rectangular finned elliptical heat exchangers with different tube arrangements," *Int. J. Heat Mass Transf.*, vol. 133, pp. 1196–1218, 2019, doi: 10.1016/j.ijheatmasstransfer.2018.12.138.

[25] B. Lotfi and B. Sundén, "Development of new finned tube heat exchanger: Innovative tube-bank design and thermohydraulic performance," *Heat Transf. Eng.*, vol. 41, no. 14, pp. 1209–1231, 2020, doi: 10.1080/01457632.2019.1637112.

[26] L. Tang, X. Du, J. Pan, and B. Sundén, "Air inlet angle influence on the air-side heat transfer and flow friction characteristics of a finned oval tube heat exchanger," *Int. J. Heat Mass Transf.*, vol. 145, p. 118702, 2019, doi: 10.1016/j.ijheatmasstransfer.2019.118702.

[27] S. He, X. Zhou, F. Li, H. Wu, Q. Chen, and Z. Lan, "Heat and mass transfer performance of wet air flowing around circular and elliptic tube in plate fin heat exchangers for air cooling," *Heat Mass Transf.*, vol. 55, no. 12, pp. 3661–3673, 2019, doi: 10.1007/s00231-019-02683-1.

[28] S. Dogan, S. Darici, and M. Ozgoren, "Numerical comparison of thermal and hydraulic performances for heat exchangers having circular and elliptic cross-section," *Int. J. Heat Mass Transf.*, vol. 145, pp. 118731, 2019, doi: 10.1016/j.ijheatmasstransfer.2019.118731.

[29] C. K. Mangrulkar, A. S. Dhoble, P. K. Pant, N. Kumar, A. Gupta, and S. Chamoli, "Thermal performance escalation of cross flow heat exchanger using in-line elliptical tubes," *Exp. Heat Transf.*, pp. 1–26, 2019, doi: 10.1080/08916152.2019.1704946.

[30] T. A. Tahseen, M. Ishak, and M. M. Rahman, "An experimental study of heat transfer and friction factor characteristics of finned flat tube banks with in-line tubes configurations," *in Applied Mechanics and Materials.*, 2014, vol. 564, pp. 197-203.

[31] T. Kim, "Effect of longitudinal pitch on convective heat transfer in crossflow over in-line tube banks," *Ann. Nucl. Energy.*, vol. 57, pp. 209–215, 2013, doi: 10.1016/j.anucene.2013.01.060.

[32] D. Sahel, H. Ameur, and M. Mellal, "Effect of tube shape on the performance of a fin and tube heat exchanger," *J. Mech. Eng. Sci.*, vol. 14, no. 2, pp. 6709-6718, 2020, doi: 10.15282/jmes.14.2.2020.13.0525.

[33] D. Sahel, H. Ameur, and W. Boudaoud, "A new correlation for predicting the hydrothermal characteristics over flat tube banks," *J. Mech. Energy Eng.*, vol. 3, no. 3, pp. 273--280, 2019, doi: 10.30464/jmee.2019.3.3.273.

[34] L. Baoxing and C. Zuhui, "Heat transfer and draft loss performance of air flowing across staggered banks of oval tubes fitted with rectangular fins," *J. Eng. Thermophys.*, vol. 4, pp. 365–371, 1982.

[35] L. Zhao, X. Gu, L. Gao, and Z. Yang, "Numerical study on airside thermal-hydraulic performance of rectangular finned elliptical tube heat exchanger with large row number in turbulent flow regime," *Int. J. Heat Mass Transf.*, vol. 114, pp. 1314–1330, 2017, doi: 10.1016/j.ijheatmasstransfer.2017.06.049.